International Journal of Thermal Sciences 88 (2015) 96–109

Contents lists available at ScienceDirect

International Journal of Thermal Sciences

journal homepage: www.elsevier.com/locate/ijts

A new parameter for the dynamic analysis of building walls using the harmonic method

G. Oliveti, N. Arcuri, D. Mazzeo, M. De Simone*

Department of Mechanical, Energy and Management Engineering, University of Calabria, P. Bucci 46/C, 87036 Rende, CS, Italy

ARTICLE INFO

Article history:
Received 13 September 2013
Received in revised form
23 June 2014
Accepted 13 September 2014
Available online 18 October 2014

Keywords:
Harmonic method
Dynamic analysis
Building walls
Thermal parameters
Time lag
Decrement factor

ABSTRACT

The authors propose a methodology to schematize correctly the capacitive effects in the transmission of heat in the multilayered walls of buildings.

An analytical study is presented related to a steady periodic regime allowing consideration of three external loads acting singularly or simultaneously: air temperature, apparent sky temperature and incident solar irradiation.

Such a study is applied in the case of four traditional types of wall (A – brick wall, B – hollow wall, C – polarized brick wall, D – prefabricated wall).

The expression of the oscillating heat flux, which penetrates the internal environment, and the conductive heat flux which penetrates the wall in contact with the external air, was obtained by means of the electrical analogy and the resolution of the equivalent circuit. It is demonstrated that the nondimensional periodic global transmittance, the ratio between the heat flux which is transferred to the indoor environment and the external heat flux, with the plant turned on, is the most suitable nondimensional parameter for the dynamic analysis of the walls. This parameter allows for the evaluation of all the typical dynamic quantities for the complete description of the thermal behavior of the walls.

1. Introduction

In the air-conditioning of buildings, the spread of cooling systems has determined a significant increase in annual energy requirement. In order to contain the energy consumption, as indicated by the recent regulations regarding energy efficiency [1,2], it is necessary to improve the thermal performance of the building shell and use more efficient plant systems. In many cases the evaluation of heat fluxes, through the external components of the building shell, is carried out with simplified procedures when one is interested in the determination of energy uses [3], while plants dimensioning requires the determination of the peak powers, which are obtained using calculation codes which can simulate the effective behavior of the building air conditioning system in dynamic conditions.

Often, during the preliminary phase of thermal design and the performance evaluation and diagnosis of buildings, the use of simplified models results as being convenient [4,5]. In Refs. [6,7] it is highlighted how, in the formulation of simplified models, it is important to correctly schematize the thermal capacitive effects and identify the parameters necessary to describe accurately the phenomena of thermal exchange and storage.

A further issue, which can arise during the planning phase, consists in the evaluation of the influence of the stratigraphical composition of the walls on the dynamic properties of the building shell [8,9]. In Refs. [10–13] the time lag and the decrement factor of a wall are determined by varying the thermophysical properties of the materials, the thickness and the position of the insulation layer, considering the sol-air temperature as the external load with a sinusoidal trend equal to 24 h. A similar approach was adopted in Ref. [14] in which an analytical study on the influence of the color, or rather of the optical properties, of the external surfaces of a building component on the transfer of heat in a steady periodic regime is presented.

A sophisticated model that takes into account the heat transfer and moisture transfer in walls whose layers are made with nonhomogeneous materials is shown in Ref. [15].

In Refs. [16,17] traditional methods for the resolution of the conduction equation (numerical methods, harmonic methods, response factor methods and methods based on conduction transfer functions (CTF)) are compared, and the advantages and disadvantages of each method are shown.

* Corresponding author. Tel.: +39 0984 494064.
E-mail addresses: marilenade_simone@yahoo.it, marilena.desimone@unical.it (M. De Simone).

http://dx.doi.org/10.1016/j.ijthermalsci.2014.09.006
1290-0729/

In particular, the harmonic method presents the advantage of providing analytical expressions of the parameters which identify the dynamic behavior of the building components. Such a setting is found in recent Standards such as EN ISO 13792:2012 [18] and EN ISO 13786:2010 [19]. The latter uses harmonic analysis in a steady periodic regime for the dynamic characterization of building components. The boundary conditions on the two faces which delimit the wall are temperature or heat flux that vary sinusoidally.

The shell walls are generally subjected to variable loads over time, prevalently due to the external air temperature, to the incident solar radiation and to the infrared radiation from the sky. From a mathematical standpoint, it is possible to approximate the variation law of such loads over time as the sum of infinite contributions (harmonics) whose variations are sinusoidal over different periods. The first is called fundamental harmonic and has period $P = 24$ h; the successive ones have $P_k = P/k$ with k integer.

The resolution of the general equation of conduction is obtained in the entire domain and, by means of the heat transfer matrix, allows the calculation of the complex amplitudes of the temperature and the heat flux on the internal side, starting from the complex amplitudes of the loads which act on the external surface.

The characteristics used are the periodic thermal admittances and the properties of dynamic heat transfer; specifically, the periodic thermal admittance correlates the oscillating heat flux with the oscillation of the temperature on the same face of the component, while the dynamic heat transfer properties correlate the oscillations of a quantity on a face of the component with the corresponding one on another face.

Among the dynamic heat exchange properties, the Standard [19] considers the periodic thermal transmittance, a complex number which provides the decrement factor of the amplitude of the oscillation and the time lag to which the load is subjected when it crosses the component. The periodic thermal admittances and transmittance are used to determine the areal heat capacity which quantifies the storage properties. It is possible to define an admittance and a thermal capacity on each side for each component.

In this work, the dynamic characterization of the walls, in steady periodic regime, is widened through the consideration of three distinct loads: the external air temperature, the apparent sky temperature and the incident solar radiation. Moreover, a dynamic analysis of the building component is developed considering the joint action of the three periodic loads, with the formulation of a matrix expression, obtained by means of the electrical analogy and the overlapping of the causes and effects, which permits the calculation of the heat flux which appears within the indoor environment when the three loads act externally.

The procedure was specially created and used in order to identify further characteristic dynamic parameters, with the aim of describing the heat transfer phenomena in a more complete manner.

Verification of the results obtained with the analytical procedure was carried out by means of a numerical model of the wall using the finite difference method.

The external loads trend was obtained starting from the experimental data of the external variables, air temperature, solar irradiation and sky temperature, recorded in clear sky conditions.

2. Methodology

The experimental values of each external load are expressed in an analytical form through a discrete Fourier series [20] with interruption of the tenth harmonic, which approximates the data by a mean steady value and a sum of sinusoids of different frequencies, amplitude and argument according to the equation:

$$y(t) = \bar{y} + \sum_{k=1}^{10} \tilde{y}_k = \bar{y} + \sum_{k=1}^{10} |\tilde{y}_k| \sin(k\omega t + \psi_k) \tag{1}$$

in which $\bar{y}$ represents the mean value, $\tilde{y}_k$ the amplitude, $k\omega$ the angular frequency and ψ_k the argument of the k-th harmonic. Fig. 1 reports the experimental data of the loads and the trends, obtained by setting the angular frequency ω equal to 0.262 rad/s, corresponding to a period of 24 h, and the steady value equal to the mean in the entire period.

In Tables 1–3 the mean value and the characteristic parameters of the first ten harmonics are reported.

Starting from the entering signals and the transfer matrix of the wall, the symbolic or phasors method is applied which, for each generic harmonic $\tilde{y}_k$ supposes the entering signal as an imaginary part of the more general signal [21]:

$$\hat{y}_k = |\hat{y}_k|[\cos(k\omega t + \psi_k) + j\mathrm{sen}(k\omega t + \psi_k)] = |\hat{y}_k| e^{j(k\omega t + \psi_k)} \tag{2}$$

Once the exiting signal has been obtained in its complex form, it is necessary to multiply it by the complex operator $e^{jk\omega t}$ and select solely the imaginary part, which forms the solution for the generic harmonic of angular frequency $k\omega$. By summing the responses obtained for the various harmonics, and adding the term relative to the null angular frequency component (steady conditions), the response to the entering signal, of which the Fourier finite series was initially broken down, is obtained.

Therefore, an entering fixed sinusoid is first transformed into a complex form and then multiplied by the transfer matrix of the same period, in order to obtain the corresponding exiting sinusoid in a complex form. In order to pass from a complex domain to a time domain, it is necessary to consider the imaginary part of this result.

3. Analysis of the dynamic response of a wall to single loads

The Standard EN ISO 13786:2010 [19] exemplifies the dynamic characterization of building components considering the external air temperature of a period equal to 24 h as a load. The convective-radiative heat transfer coefficient for internal and external surface heat exchanges are used for these evaluations. In the present work, a more accurate investigation is developed and the characterization of the building component is obtained considering the three loads and effective boundary conditions on the external surface singularly, whereas on the internal surface the thermal exchange was modeled by means of the surface heat coefficient.

For each load, the contribution of a single harmonic is evaluated considering the relation between the complex amplitudes of the temperature and of the heat flux inside and those corresponding which act on the outside [22]. The expressions obtained are:

a) external air temperature (“ea” load)

$$\begin{vmatrix} \hat{T}_{\mathrm{ia,ea}} \\ \hat{\varphi}_{i,\mathrm{ea}} \end{vmatrix} = \begin{bmatrix} 1 & -\frac{1}{h_i} \\ 0 & 1 \end{bmatrix} [Z] \begin{bmatrix} 1 & -\frac{1}{h_{e,c}} \\ 0 & 1 \end{bmatrix} \begin{vmatrix} \hat{T}_{\mathrm{ea}} \\ \hat{\varphi}_{e,c} \end{vmatrix} = \begin{bmatrix} S_{11,\mathrm{ea}} & S_{12,\mathrm{ea}} \\ S_{21,\mathrm{ea}} & S_{22,\mathrm{ea}} \end{bmatrix} \begin{vmatrix} \hat{T}_{\mathrm{ea}} \\ \hat{\varphi}_{\mathrm{e,c}} \end{vmatrix} = S_{\mathrm{ea}} \begin{vmatrix} \hat{T}_{\mathrm{ea}} \\ \hat{\varphi}_{\mathrm{e,c}} \end{vmatrix} \tag{3}$$

b) apparent sky temperature (“*sky*” load)

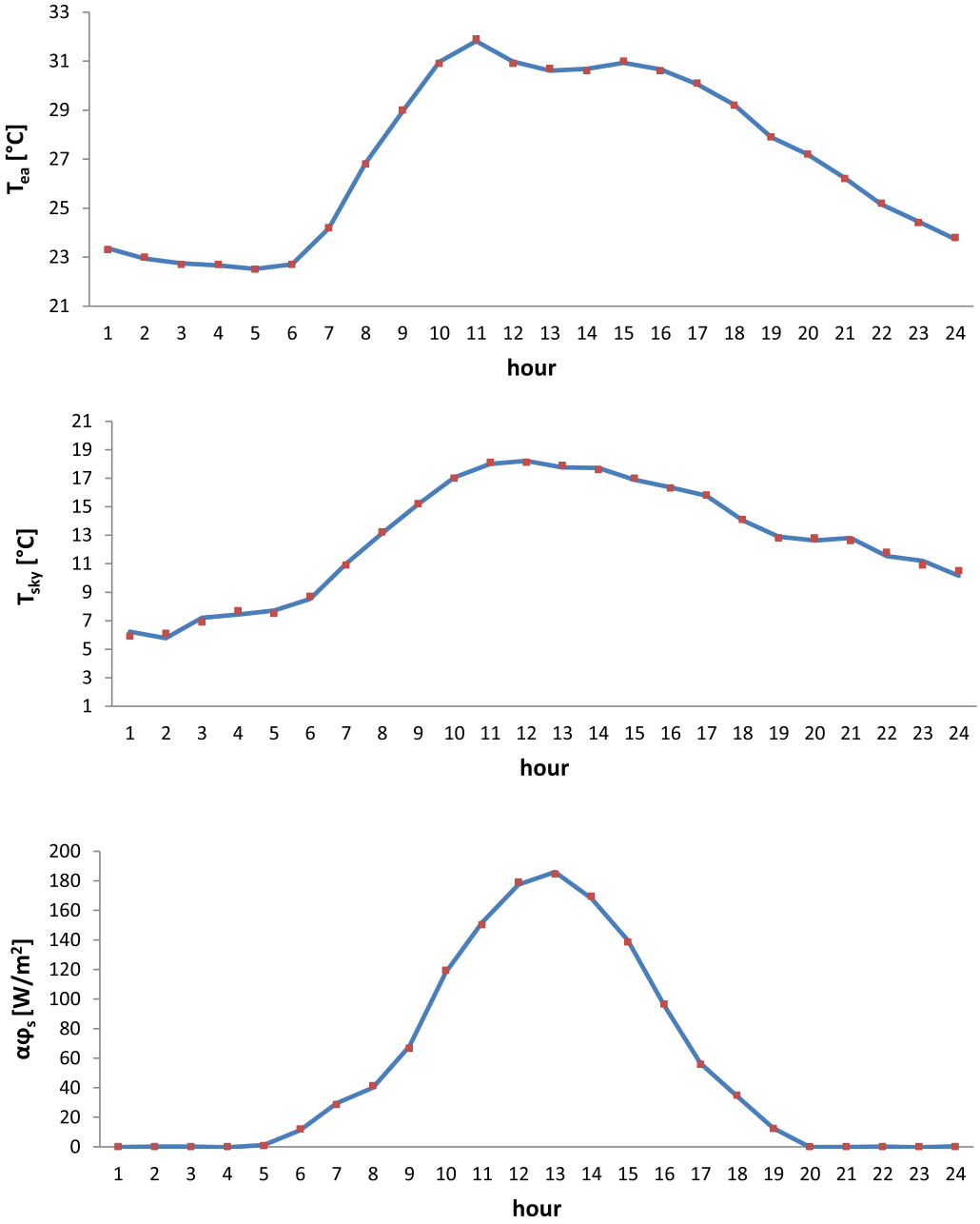

Fig. 1. Experimental trends of the loads: external air temperature T_{ea}, apparent sky temperature T_{sky} and absorbed solar irradiation $\alpha\varphi_s$ (solar absorption coefficient $\alpha = 0.40$).

$$\begin{bmatrix} \widehat{T}_{ia,sky} \\ \widehat{\varphi}_{i,sky} \end{bmatrix} = \begin{bmatrix} 1 & -\frac{1}{h_i} \\ 0 & 1 \end{bmatrix} [Z] \begin{bmatrix} 1 & -\frac{1}{h_{e,r}} \\ 0 & 1 \end{bmatrix} \begin{bmatrix} \widehat{T}_{sky} \\ \widehat{\varphi}_{e,r} \end{bmatrix} = \begin{bmatrix} S_{11,sky} & S_{12,sky} \\ S_{21,sky} & S_{22,sky} \end{bmatrix} \begin{bmatrix} \widehat{T}_{sky} \\ \widehat{\varphi}_{e,r} \end{bmatrix} = S_{sky} \begin{bmatrix} \widehat{T}_{sky} \\ \widehat{\varphi}_{e,r} \end{bmatrix} \quad (4)$$

c) solar irradiation ("s" load)

$$\begin{bmatrix} \widehat{T}_{ia,s} \\ \widehat{\varphi}_{i,s} \end{bmatrix} = \begin{bmatrix} 1 & -\frac{1}{h_i} \\ 0 & 1 \end{bmatrix} [Z] \begin{bmatrix} \widehat{T}_{2,s} \\ \alpha\widehat{\varphi}_s \end{bmatrix} = \begin{bmatrix} S_{11,s} & S_{12,s} \\ S_{21,s} & S_{22,s} \end{bmatrix} \begin{bmatrix} \widehat{T}_{2,s} \\ \alpha\widehat{\varphi}_s \end{bmatrix} = S_s \begin{bmatrix} \widehat{T}_{2,s} \\ \alpha\widehat{\varphi}_s \end{bmatrix} \quad (5)$$

The heat transfer matrix of the multilayered wall from surface to surface is:

$$[Z] = [Z_N], \ldots, [Z_1] \quad (6)$$

where $[Z_1]$, …, $[Z_N]$, are the heat transfer matrices of the various layers of the wall of the building, beginning from layer 1. As a convection for building envelope components, layer 1 shall be the outermost layer.

The matrix elements Z_{mn} of a generic layer are calculated as follows:

$$Z_{11} = Z_{22} = \cosh(\xi)\cos(\xi) + j\sinh(\xi)\sin(\xi) \quad (7)$$

Table 1
External air temperature. Mean value $\overline{T}_{ea}$, amplitude and argument of the first ten harmonics $\tilde{T}_{ea}$.

$\overline{T}_{ea}$ [°C]	26.98			
$\tilde{T}_{ea}$ [°C]	ω [rad/s]	P [h]	$\lvert\tilde{T}_{ea}\rvert$ [°C]	ψ [h]
1	0.262	24.0	−4.52	3.80
2	0.524	12.0	0.85	4.01
3	0.786	8.0	0.73	0.06
4	1.048	6.0	−0.43	0.65
5	1.310	4.8	0.10	0.64
6	1.572	4.0	0.04	1.41
7	1.834	3.4	0.12	0.17
8	2.096	3.0	−0.08	0.24
9	2.358	2.7	−0,0.05	−0.29
10	2.620	2.4	−0.08	0.75

$$Z_{12} = -\frac{\delta}{2\lambda}\{\sinh(\xi)\cos(\xi) + \cosh(\xi)\sin(\xi) + j[\cosh(\xi)\sin(\xi) - \sinh(\xi)\cos(\xi)]\} \tag{8}$$

$$Z_{21} = \frac{\lambda}{\delta}\{\sinh(\xi)\cos(\xi) - \cosh(\xi)\sin(\xi) + j[\cosh(\xi)\sin(\xi) + \sinh(\xi)\cos(\xi)]\} \tag{9}$$

with λ thermal conductivity and ξ ratio of the thickness of the layer d to the periodic penetration depth δ, given by the relation

$$\xi = \frac{d}{\delta} = \frac{d}{\sqrt{\frac{aP}{\pi}}} \tag{10}$$

with P period of oscillation and a thermal diffusivity.

The heat transfer matrix from environment to environment S_{ea}, S_{sky} and S_s are determined by the thermophysical properties of the material, by the external convective and radiative heat transfer coefficients, $h_{e,c}$ and $h_{e,r}$, by the internal heat transfer coefficient h_i and are calculated for each harmonic contribution.

In the case in which the temperature within the environment is constant and controlled by an air-conditioning plant, the amplitude of the oscillation is null and the preceding equation systems provide, for the heat flux φ_i, respectively the following equations:

$$\widehat{\varphi}_{i,ea} = -\frac{1}{S_{12,ea}}\widehat{T}_{ea} = Y_{12,ea}\widehat{T}_{ea} \tag{11}$$

$$\widehat{\varphi}_{i,sky} = -\frac{1}{S_{12,sky}}\widehat{T}_{sky} = Y_{12,sky}\widehat{T}_{sky} \tag{12}$$

Table 2
Apparent sky temperature. Mean value $\overline{T}_{sky}$, amplitude and argument of the first ten harmonics $\tilde{T}_{sky}$.

$\overline{T}_{sky}$ [°C]	12.73			
$\tilde{T}_{sky}$ [°C]	ω [rad/s]	P [h]	$\lvert\tilde{T}_{sky}\rvert$ [°C]	Ψ [h]
1	0.262	24.0	−5.36	−0.85
2	0.524	12.0	−1.47	−0.47
3	0.786	8.0	−0.23	−0.11
4	1.048	6.0	−0.59	−0.37
5	1.310	4.8	−0.29	−0.23
6	1.572	4.0	−0.31	−0.30
7	1.834	3.4	−0.38	−0.43
8	2.096	3.0	−0.21	−0.26
9	2.358	2.7	0.13	0.19
10	2.620	2.4	−0.18	−0.28

Table 3
Absorbed solar irradiation. Mean value $\alpha_s\overline{\varphi}_s$, amplitude and argument of the first ten harmonics $\alpha\tilde{\varphi}_s$.

$\alpha\overline{\varphi}_s$ [W/m^2]	53.74			
$\alpha\tilde{\varphi}_s$ [W/m^2]	ω [rad/s]	P [h]	$\lvert\alpha\tilde{\varphi}_s\rvert$ [W/m^2]	ψ [h]
1	0.262	24.0	−83.68	5.25
2	0.524	12.0	37.82	2.17
3	0.786	8.0	9.26	−2.95
4	1.048	6.0	2.17	1.05
5	1.310	4.8	0.93	−0.62
6	1.572	4.0	−2.43	−7.56
7	1.834	3.4	1.22	0.55
8	2.096	3.0	1.73	0.02
9	2.358	2.7	1.69	1.32
10	2.620	2.4	0.51	0.13

$$\widehat{\varphi}_{i,s} = \frac{1}{S_{11,s}}\alpha\widehat{\varphi}_s = Y_{11,s}\alpha\widehat{\varphi}_s \tag{13}$$

The decrement factor and the time lag for the loading ea assume the form shown in the equation:

$$f_{ea} = \frac{\lvert\widehat{\varphi}_{i,ea}\rvert}{\lvert\widehat{T}_{ea}\rvert U_{ea}} = \frac{\lvert Y_{12,ea}\rvert}{U_{ea}}; \quad \Delta t_{ea} = \frac{P}{2\pi}\arg(S_{12,ea}) \tag{14}$$

with U_{ea} steady thermal transmittance of the component calculated considering only the convective heat transfer coefficient $h_{e,c}$ on the outer surface the and $|Y_{12,ea}|$ amplitude of the periodic thermal transmittance for the loading ea.

Analogously the decrement factor and the time lag for the *sky* load can be defined considering in U_{sky} only the radiative heat transfer coefficient $h_{e,r}$ on the outer surface. For the solar load, the dynamic parameters are:

$$f_s = \frac{\lvert\widehat{\varphi}_{i,s}\rvert}{\lvert\alpha\widehat{\varphi}_s\rvert} = \lvert Y_{11,s}\rvert \;; \quad \Delta t_s = \frac{P}{2\pi}\arg(S_{11,s}) \tag{15}$$

where $|Y_{11,s}|$ is the nondimensional periodic solar thermal transmittance amplitude, thus defined:

$$\lvert Y_{11,s}\rvert = \left\lvert\frac{1}{S_{11,s}}\right\rvert \tag{16}$$

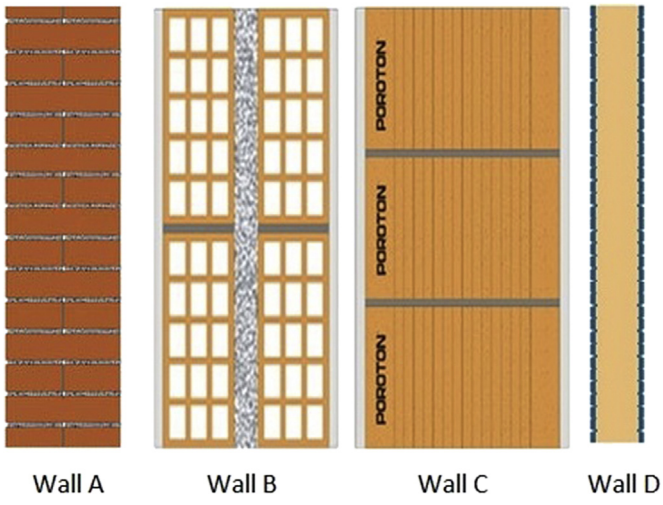

Fig. 2. Stratigraphy of the four types of walls considered.

Table 4
Type A: monolayer external wall of bricks.

	Thickness [m]	Thermal conductivity [W/m K]	Specific heat capacity [J/kg K]	Density [kg/m^3]
Brick	0.40	0.8	840	1800

Steady thermal transmittance $U = 1.494$ W/m^2 K – steady areal heat capacity $C = 604.8$ kJ/m^2 K.

For each harmonic of the single load, the preceding relations were used to determine the decrement factor and the time lag relative to four types of walls, A, B, C and D, represented in Fig. 2, and whose thermophysical properties are reported in Tables 4–7.

The boundary conditions considered are:

$$T_{ia} = T_{ia,ea} = T_{ia,sky} = T_{ia,s} = 26\ ^\circ\text{C}; \quad h_i = 7.7\frac{\text{W}}{\text{m}^2\ \text{K}};$$
$$h_{e,c} = 20\frac{\text{W}}{\text{m}^2\ \text{K}}; \quad h_{e,r} = 5.35\frac{\text{W}}{\text{m}^2\ \text{K}}$$

The radiative heat transfer coefficient on the outer surface was evaluated with an experimental investigation carried out by the authors [23].

The results obtained for the temperature loadings can be thus summarized. The temperature oscillation of the sky is more attenuated and delayed compared to that of the external air for each period considered:

$$f_{sky} < f_{ea} \quad \Delta t_{sky} > \Delta t_{ea} \tag{17}$$

If the dynamic parameters obtained for the four walls A, B, C and D are compared, the following relations are valid:

$$f_{ea,C} < f_{ea,A} < f_{ea,B} < f_{ea,D} \quad f_{sky,A} < f_{sky,C} < f_{sky,B} < f_{sky,D}$$
$$\Delta t_{ea,C} > \Delta t_{ea,A} > \Delta t_{ea,B} > \Delta t_{ea,D} \quad \Delta t_{sky,C} > \Delta t_{sky,A} > \Delta t_{sky,B} > \Delta t_{sky,D} \tag{18}$$

Wall C and wall A show the best dynamic characteristics in that they present the smallest decrement factor and the highest time lag for each harmonic.

The previous results were compared with those obtained following the methodology of the Standard, which models the external convective-radiative exchange in a different manner.

Table 8 shows the decrement factors and the time lag obtained, with reference to the fundamental harmonic $P = 24$ h and it highlights that the Standard is conservative in that it provides a higher decrement factor and a lower time lag.

It should be pointed out that such evaluations, relative to the temperature loads of the air and the sky are held to be sufficiently accurate.

Table 5
Type B: external wall with insulated hollow.

	Thickness [m]	Thermal conductivity [W/m K]	Specific heat capacity [J/kg K]	Density [kg/m^3]
External plaster	0.01	0.9	1000	1800
Brick	0.12	0.89	1000	800
Air gap	0.04			
Insulation	0.04	0.04	1450	20
Brick	0.12	0.89	1000	800
Internal plaster	0.01	0.7	1000	1400

Steady thermal transmittance $U = 0.608$ W/m^2 K – steady areal heat capacity $C = 225$ kJ/m^2 K.

Table 6
Type C: external wall in polarized brick.

	Thickness [m]	Thermal conductivity [W/m K]	Specific heat capacity [J/kg K]	Density [kg/m^3]
External plaster	0.01	0.9	840	1800
Poroton	0.38	0.17	840	630
Internal plaster	0.01	0.7	840	1400

Steady thermal transmittance $U = 0.412$ W/m^2 K – steady areal heat capacity $C = 228$ kJ/m^2 K.

The comparison among the four types of wall regarding the solar radiation was obtained by applying Eq. (13) to each individual harmonic whose characteristics are shown in Table 3. This equation evaluates the solar flux which penetrates the internal environment, set at constant temperature, starting from the solar flux absorbed by the wall on the external surface. To evaluate the contribution of the individual harmonics in the calculation of the decrement factor and that of the time lag, the external and internal heat fluxes were determined considering as well as the first harmonic, the sum of the first two, the first three, and finally the contribution of all the harmonics. Table 9 shows the decrement factors and the time lags obtained, in the case of the first harmonic with Eq. (15), and in the other cases comparing the profiles resulting from the sum of the harmonics. These profiles do not have a sinusoidal trend since they are obtained by totaling harmonics with different angular frequencies. The table shows that the greatest contribution to the decrement factor and to the time lag is to be attributed to the first harmonic whereas the contribution of the other harmonics is lower and decreases at an increase of the angular frequency. Moreover, the table shows the percentage deviation of the decrement factor and the time lag of the different compositions of the harmonics with respect to the values obtained from totaling all the harmonics.

If, for an accurate evaluation of the time lag, the fundamental harmonic and that of the period of 12 h are sufficient, in order to determine an decrement factor value which deviates at most by 2% from that which would be obtained without neglecting any harmonic contribution, it is necessary to compose the first three harmonics.

From the comparison of the dynamic parameters reported in Tables 8 and 9, it is possible to infer that the characterization of the component by means of the external air temperature loading is not

Table 7
Type D: panel for prefabricated construction.

	Thickness [m]	Thermal conductivity [W/m K]	Specific heat capacity [J/kg K]	Density [kg/m^3]
Steel	0.005	50	500	7850
Polyurethane	0.08	0.032	1400	30
Steel	0.005	50	500	7850

Steady thermal transmittance $U = 0.375$ W/m^2 K – steady areal heat capacity $C = 42.6$ kJ/m^2 K.

Table 8
Dynamic parameters f and Δt evaluated according to the Standard methodology, and parameters obtained subjecting the wall to the separate action of the external air temperature, f_{ea} and Δt_{ea}, and of the apparent temperature of the sky, f_{sky} and Δt_{sky}.

Wall type	f [–]	Δt [h]	f_{ea} [–]	Δt_{ea} [h]	f_{sky} [–]	Δt_{sky} [h]
A	0.172	12.10	0.164	12.25	0.106	13.25
B	0.512	7.02	0.500	7.21	0.328	8.71
C	0.150	14.11	0.147	14.20	0.120	15.06
D	0.980	1.32	0.978	1.38	0.947	2.08

Table 9
Incidence of the harmonics on the calculation of the decrement factor and the time lag of the solar radiation for the four types of walls.

	f_s [−]	$(f_s - f_{s,\Sigma})/f_{s,\Sigma}$ [%]	Δt_s [h]	$(\Delta t_s - \Delta t_{s,\Sigma})/\Delta t_{s,\Sigma}$ [%]
Wall A				
1	0.0354	67.39	14	7.69
Σ 1–2	0.0232	9.69	13	0
Σ 1–3	0.0214	1.41	13	0
Σ 1–10	0.0211	0	13	0
Wall B				
1	0.0490	63.96	10	11.11
Σ 1–2	0.0330	10.61	9	0
Σ 1–3	0.0303	1.31	9	0
Σ 1–10	0.0300	0	9	0
Wall C				
1	0.0199	67.33	17	0
Σ 1–2	0.0130	8.90	17	0
Σ 1–3	0.0121	1.47	17	0
Σ 1–10	0.0119	0	17	0
Wall D				
1	0.239	40.48	5	0
Σ 1–2	0.187	10.32	5	0
Σ 1–3	0.173	2.15	5	0
Σ 1–10	0.170	0	5	0

ideal to qualify the component compared to the solar load dynamically. The difference is very marked with regards to the decrement factor.

4. Dynamic analysis of a building component under the contemporaneous action of the three loads

The thermal behavior of walls which were subjected to the combined presence of the three loads, external air temperature, apparent sky temperature and absorbed solar irradiation, was studied. Reference was made to the equivalent electrical circuit in Fig. 3 which was resolved with the superposition method of the causes and effects.

The solution of the electrical circuit provides a matrix expression which links the oscillating amplitudes of the temperature and the heat flux on the internal side with the external loads T_{ea}, T_{sky} and $\alpha\varphi_s$:

$$\begin{aligned}\begin{bmatrix}\widehat{T}_{ia}\\ \widehat{\varphi}_i\end{bmatrix} &= \begin{bmatrix}1 & -\frac{1}{h_i}\\ 0 & 1\end{bmatrix}[Z]\begin{bmatrix}\frac{h_{e,r}}{h_{e,r}+h_{e,c}} & \frac{h_{e,c}}{h_{e,r}+h_{e,c}} & -\frac{1}{h_{e,r}+h_{e,c}}\\ 0 & 0 & 1\end{bmatrix}\\ &\times\begin{bmatrix}\widehat{T}_{sky}\\ \widehat{T}_{ea}\\ \widehat{\varphi}_e\end{bmatrix}+\begin{bmatrix}1 & -\frac{1}{h_i}\\ 0 & 1\end{bmatrix}[Z]\begin{bmatrix}\frac{\alpha\widehat{\varphi}_s}{h_{e,r}+h_{e,c}}\\ 0\end{bmatrix}\\ &= \begin{bmatrix}A_{11} & A_{12} & A_{13}\\ A_{21} & A_{22} & A_{23}\end{bmatrix}\begin{bmatrix}\widehat{T}_{sky}\\ \widehat{T}_{ea}\\ \widehat{\varphi}_e\end{bmatrix}+\begin{bmatrix}B_{11} & B_{12}\\ B_{21} & B_{22}\end{bmatrix}\begin{bmatrix}\frac{\alpha\widehat{\varphi}_s}{h_{e,r}+h_{e,c}}\\ 0\end{bmatrix}\\ &= [A]\begin{bmatrix}\widehat{T}_{sky}\\ \widehat{T}_{ea}\\ \widehat{T}_e\end{bmatrix}+[B]\begin{bmatrix}\frac{\alpha\widehat{\varphi}_s}{h_{e,r}+h_{e,c}}\\ 0\end{bmatrix}\end{aligned} \tag{19}$$

In the preceding relation the elements of the matrices [A] and [B] are complex numbers, and $\widehat{\varphi}_e$ represents the conductive heat flux which penetrates the wall at the interface with the external air. If the oscillating amplitude of the internal environment temperature is null, owing to the effect of the power supplied by the plant, the resolution of the equation system leads, for the internal heat flux, to the expression:

$$\begin{aligned}\widehat{\varphi}_i = &\left(A_{22}-\frac{A_{23}A_{12}}{A_{13}}\right)\widehat{T}_{ea}+\left(A_{21}-\frac{A_{23}A_{11}}{A_{13}}\right)\widehat{T}_{sky}\\ &+\left(B_{21}-\frac{B_{11}A_{23}}{A_{13}}\right)\frac{\alpha\widehat{\varphi}_s}{(h_{e,r}+h_{e,c})}\end{aligned} \tag{20}$$

It is possible to demonstrate that in Eq. (20) the multiplicative complex terms of the three loadings are a function of the periodic thermal transmittance Y_{12}, evaluated according to the Standard procedure considering only the oscillation of the external air temperature as the load. Eq. (20) can be expressed as:

$$\widehat{\varphi}_i = Y^i_{ea}\widehat{T}_{ea}+Y^i_{sky}\widehat{T}_{sky}+Y^i_s\alpha\widehat{\varphi}_s \tag{21}$$

With the parameters Y^i given by the relations:

$$Y^i_{ea} = \frac{h_{c,e}}{h_{c,e}+h_{r,e}}Y_{12} \tag{22}$$

$$Y^i_{sky} = \frac{h_{r,e}}{h_{c,e}+h_{r,e}}Y_{12} \tag{23}$$

$$Y^i_s = \frac{1}{h_{c,e}+h_{r,e}}Y_{12} \tag{24}$$

The peak power per area unit which is transferred indoors $\varphi_{i,p}$ is given by the sum of the steady component $\overline{\varphi}_i$ and by the amplitude of the fluctuating component, obtained as the maximum value of the sum of all the harmonics:

$$\varphi_{i,p} = \overline{\varphi}_i + \max_{0\le t\le P}\left(\sum_{k=1}^{10}\tilde{\varphi}_{i,k}\right) \tag{25}$$

With regards to the calculation of the energy that penetrates the indoor environment during the 24 h, it is possible to identify two cases: case (a) (Fig. 4) when the steady heat flux is greater than the maximum oscillating value in respect to the steady value and case (b) (Fig. 5) when the peak of the oscillating heat flux in respect to the steady value is greater than the steady heat flux.

In case (a) there is a compensation of the energy associated with the fluctuating components and therefore the daily energy is provided by one steady component.

In case (b) there is an inversion of the total heat flux and the total energy of the 24 h is still given by the area subtended to the steady heat flux. The total entering energy and that exiting the environment can be distinguished and can be calculated respectively with the equations:

$$E_i^+ = \frac{\overline{E}_i}{2}+\tilde{E}_i \tag{26}$$

$$E_i^- = \frac{\overline{E}_i}{2}-\tilde{E}_i \tag{27}$$

with

$$\tilde{E}_i = \int_0^P\left|\sum_{k=1}^{10}\tilde{\varphi}_{i_k}\right|dt/2 \tag{28}$$

which represent the energy associated with the fluctuating component during a half period, while $\overline{E}_i$ is the steady energy.

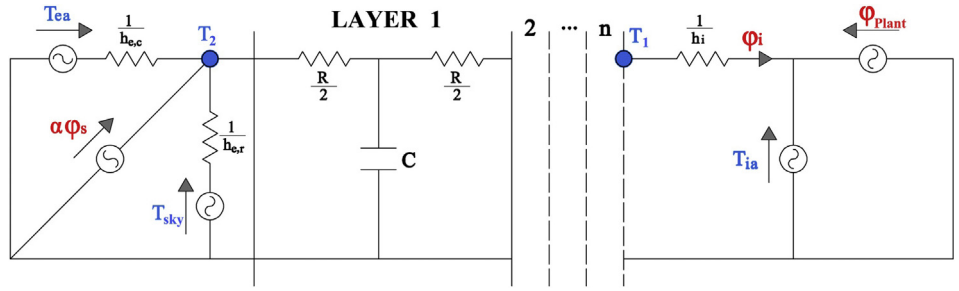

Fig. 3. Electrical circuit equivalent to a multilayer wall subject to three loads: external air temperature T_{ea}, apparent sky temperature T_{sky} and absorbed solar irradiation $\alpha\varphi_s$.

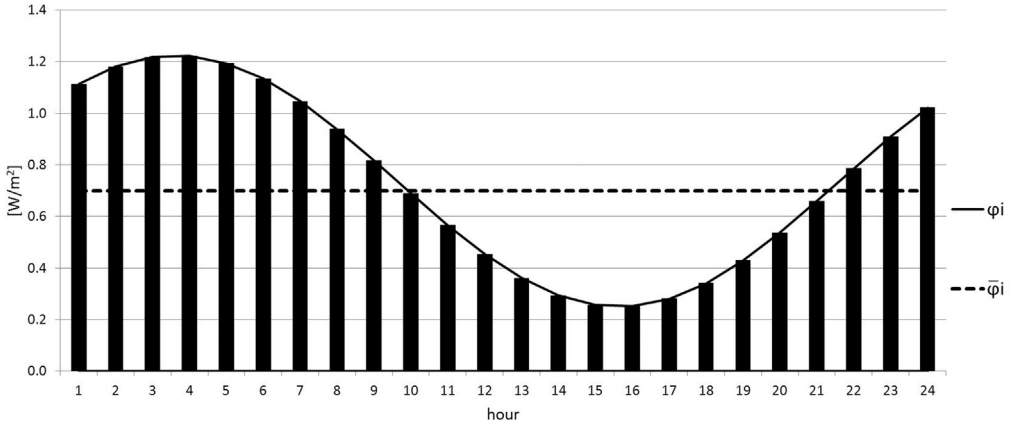

Fig. 4. Temporal trend of the total internal heat flux φ_i and of the steady heat flux $\overline{\varphi}_i$ in case (a).

Similarly, the total conductive heat flux entering the wall from the external side is equal to:

$$\widehat{\varphi}_e = Y^e_{ea}\widehat{T}_{ea} + Y^e_{sky}\widehat{T}_{sky} + Y^e_s\alpha\widehat{\varphi}_s \tag{29}$$

with the parameters $Y^e_{ea}, Y^e_{sky}, Y^e_s$, functions of the admittance on the external side Y_{22} determined according to the Standard, which can be calculated with the relations:

$$Y^e_{ea} = -\frac{h_{c,e}}{h_{c,e}+h_{r,e}}Y_{22} \tag{30}$$

$$Y^e_{sky} = -\frac{h_{r,e}}{h_{c,e}+h_{r,e}}Y_{22} \tag{31}$$

$$Y^e_s = -\frac{1}{h_{c,e}+h_{r,e}}Y_{22} \tag{32}$$

The comparison between the oscillating heat flux entering the wall (Eq. (29)) and the heat flux transferred to the indoor environment (Eq. (21)), allows for the evaluation of the decrement factor and time lag operated by the wall, while the difference between the two heat fluxes provides the variation of energy in the wall in the time unit. The following form can be given to the latter:

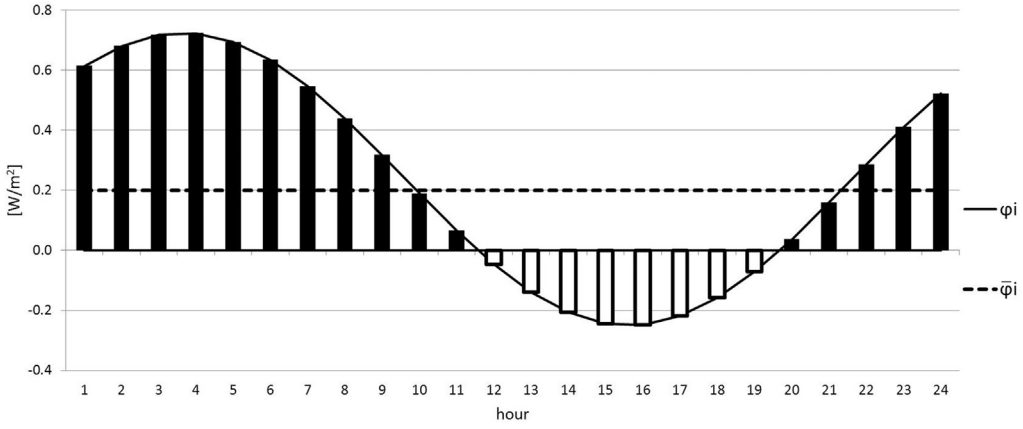

Fig. 5. Temporal trend of the total internal heat flux φ_i and of the steady heat flux $\overline{\varphi}_i$ in case (b).

$$\Delta\widehat{U} = Y^u_{ea}\widehat{T}_{ea} + Y^u_{sky}\widehat{T}_{sky} + Y^u_s\alpha\widehat{\varphi}_s \tag{33}$$

with parameters Y^u_{ae}, Y^u_c, Y^u_s, determined by the periodic areal heat capacity on the external side of the wall indicated by the Standard with κ_2:

$$Y^u_{ea} = -\frac{h_{c,e}}{h_{c,e}+h_{r,e}}\frac{2\pi}{P}\kappa_2 \tag{34}$$

$$Y^u_{sky} = -\frac{h_{r,e}}{h_{c,e}+h_{r,e}}\frac{2\pi}{P}\kappa_2 \tag{35}$$

$$Y^u_s = -\frac{1}{h_{c,e}+h_{r,e}}\frac{2\pi}{P}\kappa_2 \tag{36}$$

When the loads act externally, the building component will store a quantity of energy equal to:

$$\tilde{E}_u = \int_0^P \left|\sum_{k=1}^{10}\Delta\tilde{U}_k\right| dt/2 \tag{37}$$

Resulting from a periodic variation of all harmonics of the three loads on the external side from $-\left|\tilde{T}_{ea}\right|$ to $+\left|\tilde{T}_{ea}\right|$, from $-\left|\tilde{T}_{sky}\right|$ to $+\left|\tilde{T}_{sky}\right|$ and from $-|\alpha\tilde{\varphi}_s|$ to $+|\alpha\tilde{\varphi}_s|$ during a half period.

A schematization of the dynamic parameters, which characterize the phenomenon when the periodic variations in temperature and in heat flux on the external side have unitary dimensions, is represented in Fig. 6.

The ratio between the heat flux entering the internal environment and the conductive heat flux entering the wall, defined as the nondimensional periodic global thermal transmittance τ_G assumes the form:

$$\tau_G = \frac{\widehat{\varphi}_i}{\widehat{\varphi}_e} = \frac{Y^i_{ea}\widehat{T}_{ea} + Y^i_{sky}\widehat{T}_{sky} + Y^i_s\alpha\widehat{\varphi}_s}{Y^e_{ea}\widehat{T}_{ea} + Y^e_{sky}\widehat{T}_{sky} + Y^e_s\alpha\widehat{\varphi}_s} \tag{38}$$

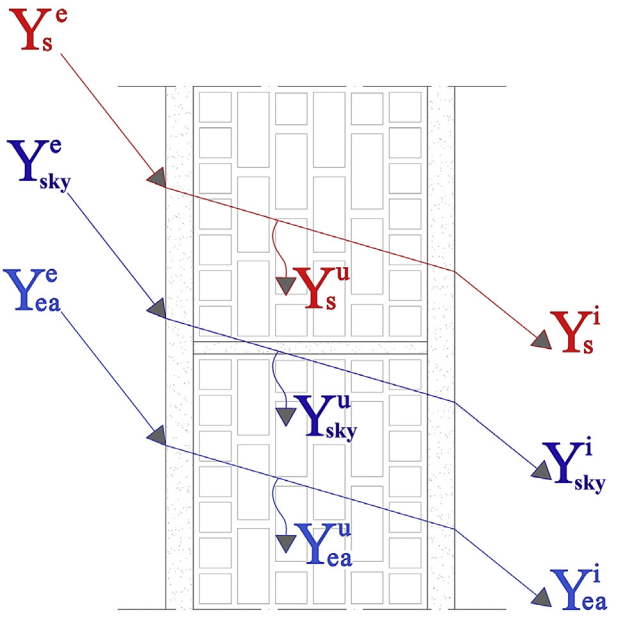

Fig. 6. Representation of the dynamic parameters which intervene in the definition of the heat fluxes on two sides of the wall and the variation in internal energy in the time unit.

The previous relations (Eqs. (22)–(24), Eqs. (30)–(32)) lead to the equalities:

$$\frac{Y^i_{ea}}{Y^e_{ea}} = \frac{Y^i_{sky}}{Y^e_{sky}} = \frac{Y^i_s}{Y^e_s} \tag{39}$$

For which the expression of the nondimensional periodic global thermal transmittance can be written as:

$$\tau_G = -\frac{Y_{12}}{Y_{22}} \tag{40}$$

In order to characterize the thermal storage capacity of the wall it can be useful to evaluate the relation between the energy accumulated in the time unit and the entering heat flux, which represents the global periodic thermal storage efficiency of the wall:

$$\varepsilon_G = \frac{\Delta\widehat{U}}{\widehat{\varphi}_e} = 1 - \tau_G = \frac{\frac{2\pi}{P}\kappa_2}{Y_{22}} \tag{41}$$

The nondimensional periodic global thermal transmittance τ_G and the storage parameter ε are evaluated using the periodic areal heat capacity κ_2 and the admittance Y_{22}, both referred to the external side, and the periodic thermal transmittance Y_{12}, calculated following the Standard procedure.

It is possible, by means of the parameter τ_G, to define the global decrement factor f_G and the global time lag Δt_G of the wall:

$$f_G = |\tau_G| \; ; \quad \Delta t_G = \frac{P}{2\pi}\arg(\tau_G) \tag{42}$$

The parameter τ_G, when calculated considering reference boundary conditions, can be used for the dynamic characterization of building components in specification of product.

Furthermore, it can be used in the dynamic thermal analysis in real use conditions for the evaluation of the oscillating heat flux $\tilde{\varphi}_i$, of the internal energy variation $\Delta\tilde{U}$ in the time unit, of the energy which is transferred to the indoor air $\tilde{E}_i$ and of the energy stored by the wall $\tilde{E}_u$.

5. Behavior of some characteristic walls

The previous relations were used in order to determine the dynamic performance of the previously defined walls subjected to the joint action of the three loads.

This required the reconstruction of the external and internal heat flux trends, by means of the composition of harmonics, in such a way as to carry out the characterization and evaluation of the performance of the walls considered.

Starting from the characteristic parameters of the different harmonics, reported in Tables 1–3, and the values of the parameters Y^i (Eqs. (22)–(24)) and the parameters Y^e (Eqs. (30)–(32)), by means of the Eqs. (21) and (29) the conductive heat flux trend entering the external side of the wall and that transferred to the inside was reconstructed.

Specifically, the time trends of the first harmonic, and the sum of the harmonics up to the fifth in order to make a comparison with the trend which is obtained considering the sum of all the oscillations, were determined. The results obtained for the external $\tilde{\varphi}_e$ and internal $\tilde{\varphi}_i$ heat flux, for the four types of walls, are reported in Fig. 7.

For all the walls, the fundamental harmonic is not sufficient to represent the trend of the conductive heat flux which penetrates the wall. It is necessary to consider at least two or more harmonics in order to obtain increased accuracy. Instead, with regards to the

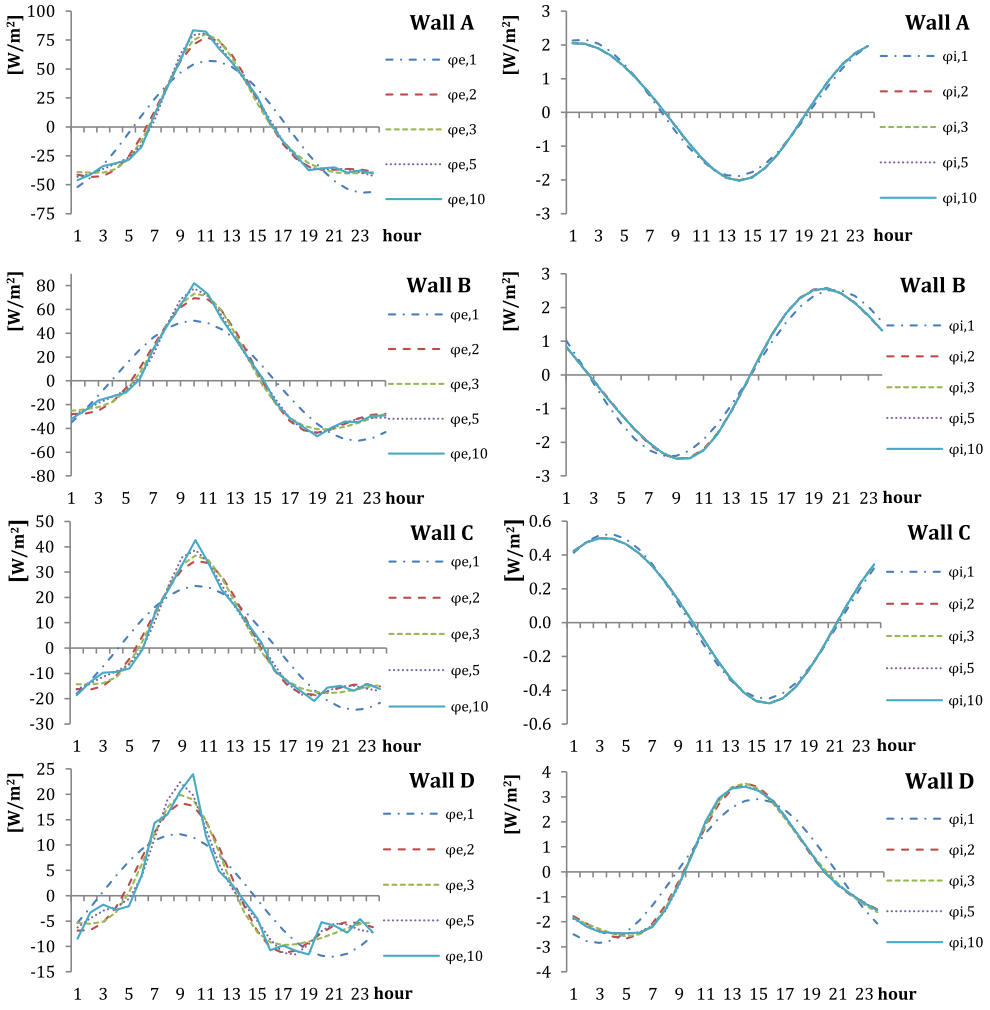

Fig. 7. Internal and external conductive heat flux trend resultant from the harmonic composition for the walls A, B, C and D considered.

internal heat flux, the use of the first two sinusoids always proves adequate.

The non dimensional periodic global thermal transmittance τ_G (Eq. (40)) and the relative dynamic parameters f_G and Δt_G (Eq. (42)) were determined for each wall.

The results obtained for each individual harmonic are compared in Table 10.

In order to obtain the effective decrement factor and time lag it is necessary to arrange the results of the previous table.

The results of the deviation of the two parameters of the effective value obtained by arranging the different harmonics are reported in Table 11.

The table shows that with the first five harmonics it is possible to obtain a deviation of the effective global decrement factor at most of 10%, whereas with regard to the effective global time lag the reconstruction proves more random, in that the first two harmonics are necessary for walls B and C, and more than five for walls D and A.

Table 10
Amplitude and argument of the non dimensional periodic global thermal transmittance τ_G for each harmonic of the considered walls.

k-th harmonic	τ_G							
	Wall A		Wall B		Wall C		Wall D	
	f_G [–]	Δt_G [h]	f_G [–]	Δt_G [h]	f_G [–]	Δt_G [h]	f_G [–]	Δt_G [h]
1	0.0354	14.31	0.0491	10.59	0.0199	17.45	0.2382	6.14
2	0.0072	9.91	0.0142	6.70	0.0029	0.30	0.1154	3.81
3	0.0022	0.002	0.0061	5.14	0.0007	2.01	0.0713	2.91
4	0.0008	0.87	0.0032	4.28	0.0002	2.64	0.0485	2.42
5	0.0003	1.31	0.0019	3.73	0.00007	2.91	0.0349	2.10
6	0.0002	1.55	0.0012	3.34	0.00002	3.02	0.0260	1.87
7	0.0001	1.69	0.0007	3.05	0.00001	3.06	0.0199	1.70
8	0.00004	1.77	0.0005	2.82	0.000004	0.06	0.0156	1.56
9	0.00002	1.82	0.0003	2.63	0.000002	0.37	0.0124	1.45
10	0.00001	1.85	0.0002	0.08	0.0000009	0.60	0.0100	1.35

From the analysis of the dynamic parameters, wall B proves to be that with the smallest global decrement factor and the highest global time lag.

The comparison between the dynamic parameter values of Tables 7 and 10 shows that the characterization of the walls in the effective conditions of use differs from that obtained only considering temperature oscillation, which provides only qualitative type indications.

The effectiveness of this analysis, for the evaluation of the dynamic performance of the walls, is shown by the comparison between the internal and external heat flux trend, obtained composing the steady heat flux with the oscillating heat flux, reported in Fig. 8.

In such a way it is possible to evaluate the instant and the peak value of the heat flux which penetrates the wall and the instant and the corresponding maximum heat flux value which is transferred to the indoor environment. Specifically, walls A and B, with higher steady thermal transmittance, prove to have a greater heat flux which penetrates from the external surface of the wall, while wall D, characterized by lower steady thermal transmittance, presents a more reduced heat flux on the external side. The heat flux which is transferred to the indoor environment is determined by the dynamic properties of the walls.

The variation of the internal energy in the time unit, formed through the sum of the various harmonic components, given that the steady component is null, is shown in Fig. 9. Also in this case, the heat storage entity is closely linked to the steady areal heat capacity and to the quantity of energy that penetrates the wall, and therefore the considerations made previously are valid.

For the walls considered, the steady and dynamic parameters necessary for the evaluation of the total energy entering and exiting the internal environment are reported in Table 12.

The comparison between the internal steady heat flux $\overline{\varphi}_i$ and the maximum heat flux associated with the oscillating components of the internal heat flux $\max_{0\le t\le P}(\sum_{k=1}^{10}\tilde{\varphi}_{i,k})$ shows that the heat flux entering into the environment through the walls considered present an inversion. The energy associated with the time interval in which the total heat flux is entering the environment was calculated with Eq. (26) and the exiting energy was calculated with Eq. (27). Table 11 shows that the steady energy $\overline{E}_i$ is notably reduced compared to the fluctuating energy in a semi-period $\tilde{E}_i$.

Wall D presents the least stored energy $\tilde{E}_u$ and the highest peak of the internal heat flux value $\max_{0\le t\le P}(\sum_{k=1}^{10}\tilde{\varphi}_{i,k})$, confirming that it is the least suitable wall during summer functioning.

Table 11
Deviations from the effective decrement factor and time lag value obtained composing the harmonics.

	f_G [−]	$(f_G - f_{G,\Sigma})/f_{G,\Sigma}$ [%]	Δt_G [h]	$(\Delta t_G - \Delta t_{G,\Sigma})/\Delta t_{G,\Sigma}$ [%]
		Wall A		
1	0.0354	53.51	15	0
Σ 1–2	0.0249	7.97	14	−6.67
Σ 1–3	0.0240	4.06	14	−6.67
Σ 1–5	0.0238	3.27	14	−6.67
Σ 1–10	0.0230	0	15	0
		Wall B		
1	0.0491	60.25	11	10
Σ 1–2	0.0362	18.38	10	0
Σ 1–3	0.0341	11.29	10	0
Σ 1–5	0.0323	5.57	10	0
Σ 1–10	0.0306	0	10	0
		Wall C		
1	0.0199	83.10	18	5.88
Σ 1–2	0.0134	23.46	17	0
Σ 1–3	0.0127	16.68	17	0
Σ 1–5	0.0120	10.11	17	0
Σ 1–10	0.0109	0	17	0
		Wall D		
1	0.2382	68.92	6	50
Σ 1–2	0.1919	36.07	5	25
Σ 1–3	0.1770	25.49	5	25
Σ 1–5	0.1524	8.07	5	25
Σ 1–10	0.1410	0	4	0

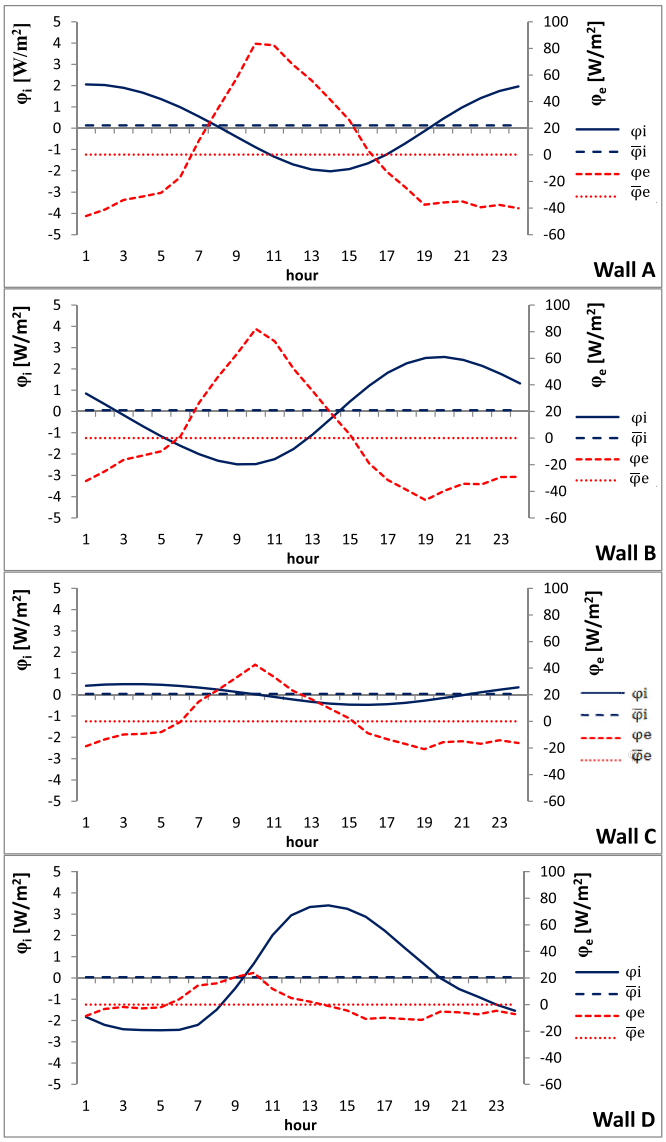

Fig. 8. Trend of the internal heat flux φ_i and of the external conductive heat flux φ_e, and value of the steady heat flux, for the four types of walls considered.

6. Comparison and validation

The dynamic model for the analysis of multilayered building components was tested by means of a finite difference numerical model. This model approximates the differential equation of monodimensional transitory thermal conduction by a system of algebraic equations of nodal thermal balance solved using the implicit method [24]. Specifically, the trends of the external heat flux entering the wall were compared with the heat flux transferred to the air-conditioned environment, calculated analytically using the previously defined dynamic parameters and numerically using a nonuniform spatial discretization that involves 18 nodes and a time-step of an hour.

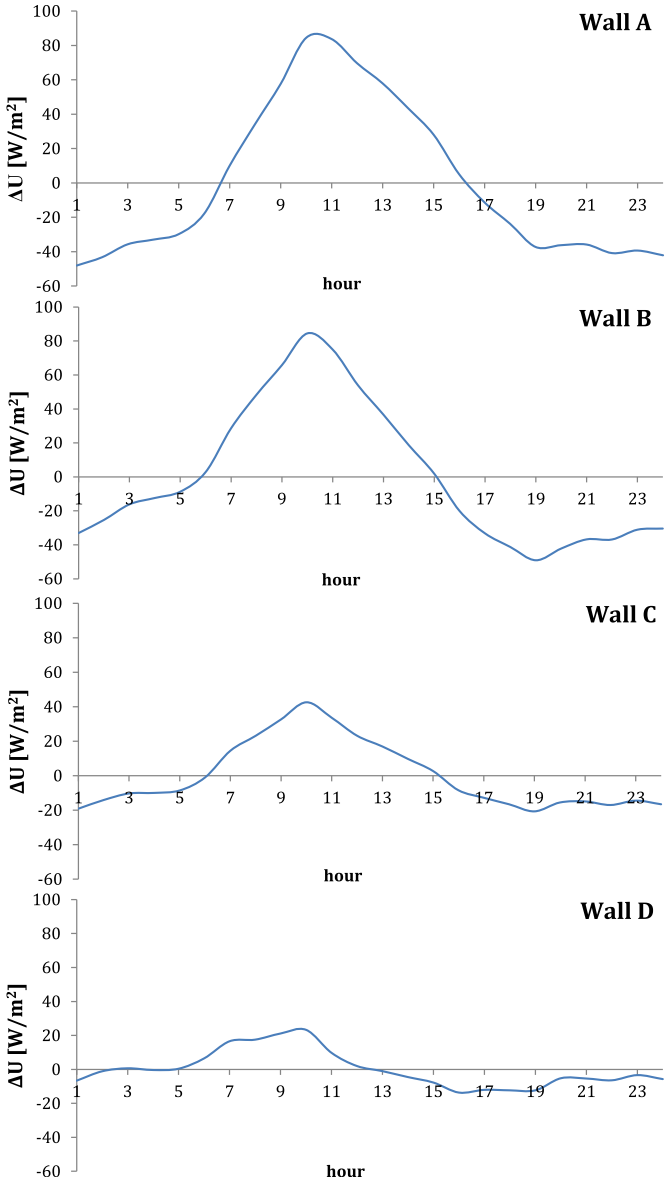

Fig. 9. Variation in the internal energy in the time unit ΔU for the four walls considered.

The comparison was made considering the wall subjected individually and simultaneously to the action of the loads T_{ea}, T_{sky} and $\alpha\varphi_s$.

As a test wall reference was made to the wall B type, representative of the residential building walls, whose characteristics are shown in Table 5.

6.1. Analysis of the dynamic response of a hollow-wall to single loadings

The analytical evaluation of the external and internal heat fluxes was obtained considering the individual loads using the relations:

a) external air temperature load

$$\varphi_{e,c} = \overline{\varphi}_{e,c} + \sum_{k=1}^{10} \tilde{\varphi}_{e,c_k} \tag{43}$$

$$\varphi_{i,ea} = \overline{\varphi}_{i,ea} + \sum_{k=1}^{10} \tilde{\varphi}_{i,ea_k} \tag{44}$$

The oscillating components were obtained solving the matrix equation Eq. (3) for each harmonic that supplies the expressions:

$$\widehat{\varphi}_{e,c} = \frac{1}{S_{22,ea}}\widehat{\varphi}_{i,ea} - \frac{S_{21,ea}}{S_{22,ea}}\widehat{T}_{ea} \tag{45}$$

$$\widehat{\varphi}_{i,ea} = -\frac{1}{S_{12,ea}}\widehat{T}_{ea} = Y_{12,ea}\widehat{T}_{ea} \tag{11a}$$

for the steady components

$$\overline{\varphi}_{e,c} = \overline{\varphi}_{i,ea} = U_{ea}\left(\overline{T}_{ea} - \overline{T}_{ia,ea}\right) \tag{46}$$

with U_{ea} previously defined.

b) apparent sky temperature load

$$\varphi_{e,r} = \overline{\varphi}_{e,r} + \sum_{k=1}^{10} \tilde{\varphi}_{e,r_k} \tag{47}$$

$$\varphi_{i,sky} = \overline{\varphi}_{i,sky} + \sum_{k=1}^{10} \tilde{\varphi}_{i,sky_k} \tag{48}$$

by solving the matrix equation Eq. (4) the following expressions are obtained for each harmonic:

$$\widehat{\varphi}_{e,r} = \frac{1}{S_{22,sky}}\widehat{\varphi}_{i,sky} - \frac{S_{21,sky}}{S_{22,sky}}\widehat{T}_{sky} \tag{49}$$

$$\widehat{\varphi}_{i,sky} = -\frac{1}{S_{12,sky}}\widehat{T}_{sky} = Y_{12,sky}\widehat{T}_{sky} \tag{12a}$$

for the steady components

$$\overline{\varphi}_{e,r} = \overline{\varphi}_{i,sky} = U_{sky}\left(\overline{T}_{sky} - \overline{T}_{ia,sky}\right) \tag{50}$$

with U_{sky} previously defined.

c) solar irradiation load

$$\varphi_{e,s} = \alpha\overline{\varphi}_s + \sum_{k=1}^{10} \alpha\tilde{\varphi}_{s_k} \tag{51}$$

$$\varphi_{i,s} = \overline{\varphi}_{i,s} + \sum_{k=1}^{10} \tilde{\varphi}_{i,s_k} \tag{52}$$

The matrix equation Eq. (4) supplies the following expression for each harmonic:

$$\widehat{\varphi}_{i,s} = \frac{1}{S_{11,s}}\alpha\widehat{\varphi}_s = Y_{11,s}\alpha\widehat{\varphi}_s \tag{13a}$$

The steady component $\alpha\overline{\varphi}_s = \overline{\varphi}_{i,s}$ is the mean of the incident solar radiation absorbed by the wall.

Figs. 10–12 show the trends of the external and internal heat fluxes calculated analytically and numerically.

Table 12
Steady internal heat flux $\overline{\varphi}_i$, maximum heat flux associated with the fluctuating components of the internal heat flux $\max_{0\le t\le P}(\sum_{k=1}^{10}\tilde{\varphi}_{i,k})$, steady energy which enters the environment $\overline{E}_i$, fluctuating energy in a semiperiod which enters the internal environment $\tilde{E}_i$, total entering energy E_i^+ and total exiting energy E_i^- in the case of inversion of the heat flux and stored energy $\tilde{E}_u$ for the four walls considered.

	Wall A	Wall B	Wall C	Wall D
$\overline{\varphi}_i$ [W/m^2]	0.136	0.055	0.037	0.034
$\max_{0\le t\le P}(\sum_{k=1}^{10}\tilde{\varphi}_{i,k})$ [W/m^2]	2.056	2.508	0.463	3.376
$\overline{E}_i$ [kJ/m^2]	11.73	4.77	3.23	2.94
$\tilde{E}_i$ [kJ/m^2]	55.79	68.47	13.44	81.44
E_i^+ [kJ/m^2]	61.65	70.86	15.06	82.91
E_i^- [kJ/m^2]	−49.93	−66.09	−11.83	−79.97
$\tilde{E}_u$ [kJ/m^2]	1706.37	1497.91	717.65	351.83

The numerical values follow perfectly the trends obtained analytically and the slight deviations can be reduced by increasing the number of nodes and reducing the integration step.

6.2. Analysis of the dynamic response of a hollow-wall under the contemporaneous action of the three loads

The relations for the calculation of the external flux φ_e and the internal flux φ_i have the form:

$$\varphi_e = \overline{\varphi}_e + \sum_{k=1}^{10}\tilde{\varphi}_{e_k} \tag{53}$$

$$\varphi_i = \overline{\varphi}_i + \sum_{k=1}^{10}\tilde{\varphi}_{i_k} \tag{54}$$

The fluctuating components $\widehat{\varphi}_e$ and $\widehat{\varphi}_i$ are obtained solving the matrix system (Eq. (19)) and are obtainable respectively using Eqs. (29) and (21).

The steady heat flux is given by the relation.

$$\overline{\varphi}_e = \overline{\varphi}_i = \frac{(\overline{T}_2 - \overline{T}_1)}{\sum R} \tag{55}$$

with $\overline{T}_1$ and $\overline{T}_2$ mean steady internal and external surface temperatures and $\sum R$ sum of the conductive resistances of the wall layers. The temperatures $\overline{T}_1$ and $\overline{T}_2$ were determined solving the electric circuit of Fig. 3 without capacitors and are equal to

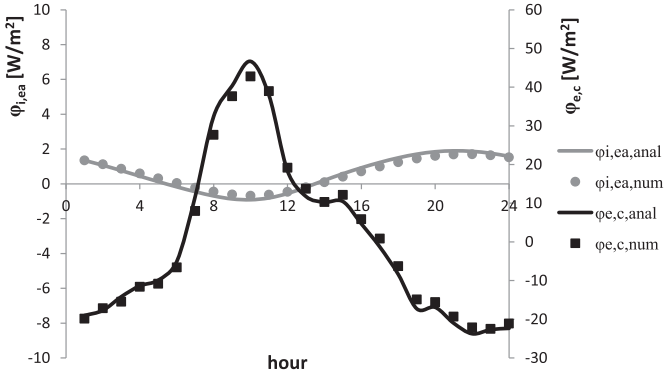

Fig. 10. External air temperature load. Comparison of the trend of the external convective heat flux with the internal heat flux calculated using the analytical model and using the numerical model.

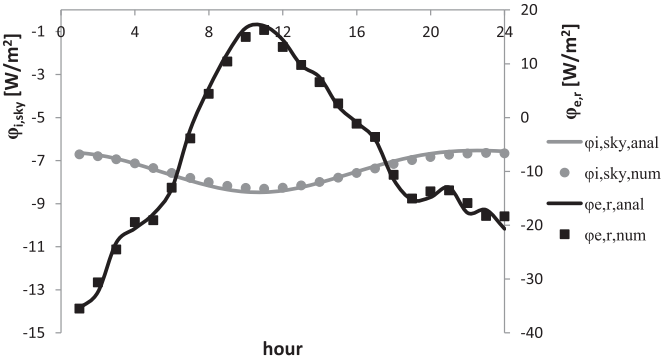

Fig. 11. Apparent sky temperature load. Comparison of the trend of the external radiative heat flux with the internal heat flux calculated using the analytical model and using the numerical model.

$$\overline{T}_1 = \frac{\alpha\overline{\varphi}_s + h_i\overline{T}_{ia} + h_{e,c}\overline{T}_{ea} + h_{e,r}\overline{T}_{sky} + h_i\overline{T}_{ia}\sum R\,(h_{e,c} + h_{e,r})}{h_i + h_{e,c} + h_{e,r} + h_i\sum R(h_{e,c} + h_{e,r})} \tag{56}$$

$$\overline{T}_2 = h_i(\overline{T}_1 - \overline{T}_{ia})\sum R + \overline{T}_1 \tag{57}$$

Fig. 13 compares the trends of the entering and exiting heat fluxes of the wall calculated analytically and numerically.

An excellent agreement is found also in this case between the two trends and this demonstrates that the analytical model and the relative dynamic parameters defined are suitable to describe the thermal behavior of the wall in real conditions of use.

7. Conclusions

An accurate analysis of the thermal behavior of external walls of buildings in a steady periodic regime by the harmonic method, considering the external air temperature, the apparent sky temperature and solar irradiation as loads, was developed.

The simplification adopted by the Standard EN ISO 13786, which provides for the schematizing of the outdoor environment by means of a temperature oscillation period equal to 24 h, does not prove adequate for the evaluation of the dynamic characteristics of the building components. For example, the characterization of solar radiation requires the determination of the nondimensional periodic solar thermal transmittance.

The evaluation of the conductive heat flux which penetrates the wall at the interface with the external air and of the heat flux which

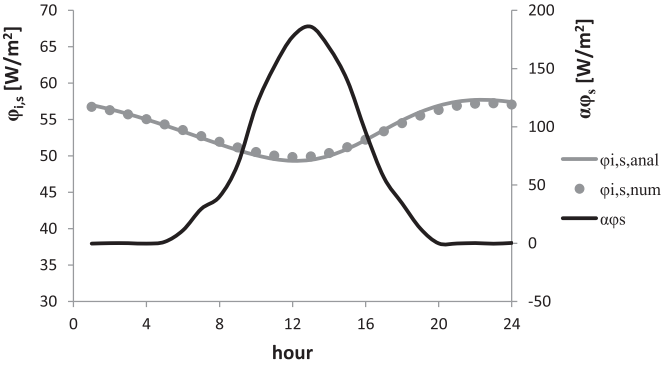

Fig. 12. Solar irradiation load. Comparison of the trend of the external absorbed solar heat flux with the internal heat flux calculated using the analytical model and using the numerical model.

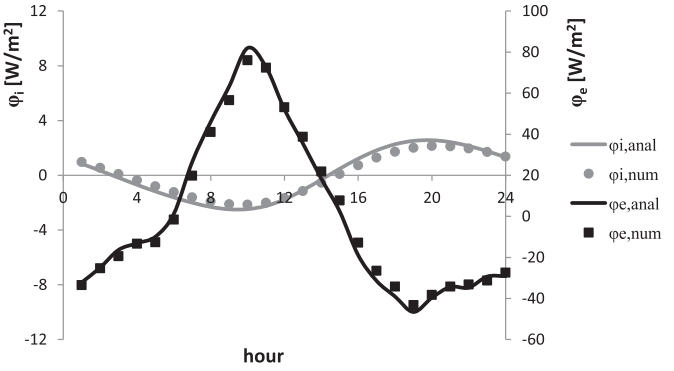

Fig. 13. Contemporaneous action of the loads T_{ea}, T_{sky}, $\alpha\varphi_s$. Comparison of the trend of the external and internal heat flux calculated using the analytical model and using the numerical model.

is transferred to the environment, by means of the simultaneous action of the three loads considered, led to the definition of the nondimensional periodic global thermal transmittance.

This parameter allows for the calculation of the global decrement factor and time lag which is undergone by the heat flux when it crosses the wall, the stored energy, the peak power which is transferred to the internal environment, and the energies which enter and exit the environment in the case of inversion of the heat flux at the internal air interface.

The analysis highlighted that the preceding quantities can be evaluated by means of the periodic areal thermal capacity and the periodic thermal admittance, both referring to the external side, and the periodic thermal transmittance, calculated considering only the external air temperature as load.

The non dimensional periodic global transmittance can be used for the characterization of building components in specifications of product and as calculation parameter in dynamic regime thermal analysis.

The newly defined parameters were used to compare the thermal performance in a dynamic regime of some types of commonly used walls.

The calculation method was tested by means of a comparison of the entering and exiting heat fluxes of a typical wall calculated analytically and numerically.

References

[1] Directive 2002/91/EC of the European Parliament and of the Council on the Energy Performance of Buildings, December 2002.
[2] Directive 2010/31/UE of the European Parliament and of the Council on the Energy Performance of Buildings (Recast), May 2010.
[3] EN ISO 13790, Energy Performance of Buildings – Calculation of Energy Use for Space Heating and Cooling, 2008.
[4] Youming Chen, Shengwei Wang, A new procedure for calculating periodic response factors based on frequency domain regression method, Int. J. Therm. Sci. 44 (2005) 382–392.
[5] Xinhua Xu, Shengwei Wang, A simplified dynamic model for existing buildings using CTF and thermal network models, Int. J. Therm. Sci. 47 (2008) 1249–1262.
[6] Shengwei Wang, Xinhua Xu, Simplified building model for transient thermal performance estimation using GA-based parameter identification, Int. J. Therm. Sci. 45 (2006) 419–432.
[7] G. Fraisse, C. Viardot, O. Lafabrie, G. Achard, Development of a simplified and accurate building model based on electrical analogy, Energy Build. 34 (2002) 1017–1031.
[8] M. Ciampi, F. Leccese, G. Tuoni, Multi-layered walls design to optimize building-plant interaction, Int. J. Therm. Sci. 43 (2004) 417–429.
[9] N. Daouas, A study on optimum insulation thickness in walls and energy savings in Tunisian buildings based on analytical calculation of cooling and heating transmission loads, Appl. Energy 88 (2011) 156–164.
[10] H. Asan, Y.S. Sancaktar, Effect of wall's thermophysical properties on time lag and decrement factor, Energy Build. 28 (1998) 159–166.
[11] H. Asan, Effect of wall's insulation thickness and position on time lag and decrement factor, Energy Build. 28 (1998) 299–305.
[12] H. Asan, Investigation of wall's optimum insulation position from maximum time lag and minimum decrement factor point of view, Energy Build. 32 (2000) 197–203.
[13] H. Asan, Numerical computation of time lags and decrement factors for different building materials, Build. Environ. 41 (2006) 615–620.
[14] A.D. Granja, L.C. Labaki, Influence of external surface colour on the periodic heat flow through a flat solid roof with variable thermal resistance, Int. J. Energy Res. 27 (2003) 771–779.
[15] J. Sykora, J. Vorel, T. Krejci, M. Sejnoha, J. Sejnoha, Analysis of coupled heat and moisture transfer in masonry structures, Mater. Struct. 42 (2009) 1153–1167.
[16] Changhai Peng, Zhishen Wu, Thermoelectricity analogy method for computing the periodic heat transfer in external building envelopes, Appl. Energy 85 (2008) 735–754.
[17] F. Varela, F.J. Rey, E. Velasco, S. Aroca, The harmonic method: a new procedure to obtain wall periodic cross response factors, Int. J. Therm. Sci. 58 (2012) 20–28.
[18] EN ISO 13792, Thermal Performance of Buildings – Calculation of Internal Temperatures of a Room in Summer Without Mechanical Cooling – Simplified Methods, 2012.
[19] EN ISO 13786, Thermal Performance of Buildings Components – Dynamic Thermal Characteristics – Calculation Methods, 2010.
[20] M.G. Smart, J.A. Ballinger, Fourier-synthesized weather data for building energy use estimation, Build. Environ. 19 (1984) 41–48.
[21] E. Kreyszig, Advanced Engineering Mathematics, seventh ed., John Wiley & Sons, Inc., Singapore, 1993.
[22] H.S. Carslaw, J.C. Jaeger, Conduction of Heat in Solids, second ed., Oxford Science Publications, 1988.
[23] G. Oliveti, N. Arcuri, M. De Simone, R. Bruno, Experimental evaluations of the building shell radiant exchange in clear sky conditions, Sol. Energy 86 (2012) 1785–1795.
[24] W.M. Rohhsenow, J.P. Hartnett, Handbookof Heat Transfer, Mc Graw Hill Book Company, USA, 1973.

Nomenclature

a: thermal diffusivity [m^2/s]
[A]: heat transfer matrix considering the contemporaneous action of the three loads
[B]: heat transfer matrix considering the contemporaneous action of the three loads
C: steady areal heat capacity [J/m^2 K]
d: thickness of the layer [m]
E: thermal energy [J/m^2]
f: decrement factor [−]
h: heat transfer coefficient [W/m^2 K]
k: harmonic order [−]
P: period of oscillation [s]
R: thermal resistance [m^2 K/W]
S_{mn}: element of the heat transfer matrix from environment to environment considering the individual loads
t: time [s]
T: temperature [K]
U: steady thermal transmittance [W/m^2 K]
y: thermal quantity
Y_{22}: periodic thermal admittance on external side wall [W/m^2 K]
Y_{11}: non dimensional periodic solar thermal transmittance [−]
Y_{12}: periodic thermal transmittance [W/m^2 K]
[Z]: heat transfer matrix of the multilayered wall from surface to surface
Z_{mn}: element of the heat transfer matrix of a generic layer

Greek symbols

α: absorption coefficient [−]
δ: periodic penetration depth of a heat wave in a material [m]
Δt: time lag [s]
ΔU: instantaneous internal energy variation [W/m^2]
ε: periodic efficiency of thermal accumulation [−]
κ: periodic areal heat capacity [J/m^2 K]
λ: thermal conductivity [W/m K]
ξ: ratio of the thickness of the layer to the periodic penetration depth [−]
τ: non dimensional periodic thermal transmittance [−]
φ: heat flux [W/m^2]
ψ: argument of the thermal quantity oscillation [rad]
ω: angular frequency of the variations [rad/s]

Subscripts

anal: analytical
A: brick wall
B: hollow wall
c: convective
C: polarized brick wall

D: prefabricated wall
e: external
ea: referring to the external air loading
G: global, referred to the three loadings
i: internal
ia: internal air
k: *k*-th harmonic
m: *m*-th row
n: *n*-th column
N: *N*-th layer
num: numerical
p: peak value
Plant: plant
r: radiative
s: referring to the solar load
sky: referring to the sky load
Σ: referring to the sum of all the harmonics
1: internal side wall
2: external side wall

Superscripts

+: entering
−: outgoing
e: external
i: internal
u: accumulated

Symbols

−: mean value
~: oscillating value in the time domain
^: oscillating value in the complex domain
||: amplitude of an oscillating value
arg: argument of an oscillating value